Exciton lifetime in donor-acceptor-donor planar dumbbell-shaped triazatruxene-thienopyrroledione derivatives

Jiang Jing, Émilie Steveler, Nicolas Leclerc, Anthony d'Aléo, Benoit Heinrich, Wilfried Uhring, Thomas Heiser

Exciton lifetime in donor-acceptor-donor planar dumbbell-shaped triazatruxene-thienopyrroledione derivatives

Jiang Jing[a], Emilie Steveler[*a], Nicolas Leclerc[b], Anthony D'Aléo[c], Benoît Heinrich[c], Wilfried Uhring[c], Thomas Heiser[a]

[a]ICube Research Institute, Université de Strasbourg, CNRS, INSA-Strasbourg, UMR 7357, 23 rue du Loess, 67037 Strasbourg, France; [b]Institut de Chimie et Procédés pour l'Energie, l'Environnement et la Santé Université de Strasbourg, CNRS, UMR 7515, 25 rue Becquerel, 67087 Strasbourg, France; [c]Institut de Physique et Chimie des Matériaux de Strasbourg, Université de Strasbourg, CNRS, UMR 7504, 23 rue du Loess, 67034 Strasbourg, France

ABSTRACT

Organic semiconductor materials such as planar conjugated small molecules are of great interest to the photovoltaic community. In thin films, the exciton and charge carrier dynamics, which are crucial to photovoltaic device operation, depend in a non-trivial way on the organic molecular structure and on the molecular organization in the solid state. Recently, the exciton diffusion has been found to strongly depend on the crystalline order of the organic thin films. This work presents the study of the exciton lifetime in an innovative class of molecular semiconductors able to present different crystalline order. This family of molecules has a "dumbbell-shaped" structure based on triazatruxene units that act as a π-stacking platform. Such molecules with different side-chains have been found to self-assemble into various crystalline and liquid crystalline phases. We have studied the steady-state photoluminescence and the exciton lifetime for several triazatruxene-based derivatives with different side-chains, in solution and in thin films for different solid state phases. In solution, the fluorescence lifetime corresponds to the reference value that can be obtained without intermolecular interaction. In thin films, we measured the exciton lifetime for different molecular structures in order to correlate the exciton dynamics with the molecular stacking. The results reveal a significant increase in the exciton lifetime with the enhancement of the structural order.

Keywords: exciton dynamics, exciton lifetime, molecular semiconductor, self-assembly.

1. INTRODUCTION

Exciton dynamics play an essential role in organic photovoltaic (OPV) devices. Indeed, most OPV devices rely on singlet excitons, whose lifetime is generally of the order of nanoseconds (ns) and whose diffusion length is estimated to be less than 10 nm, which limit the power conversion efficiency (PCE) of OPV devices[1, 2]. To avoid this restriction and allow high proportion of excitons to reach the donor/acceptor interface, it is necessary to use a bulk heterojunctions (BHJ) structure, whose morphology is determinant, but still difficult to control[3, 4].There have been multiple efforts to understand what factors limit the singlet exciton diffusion in the solid state and to figure out ways to enhance it. Improving the exciton diffusion length, and importantly, increasing exciton lifetime is essential. One strategy has been to enhance exciton lifetime by improving the structural order of molecular solid-states. In this case, planar conjugated small molecules are of interest as they have a strong ability to form ordered solid-states[5-11].

Here, we present the study of the exciton lifetime in a family of planar conjugated small molecules, called TPD-TAT. TPD-TAT derivatives share the same conjugated "donor-acceptor-donor" backbone with a thienopyrroledione (or "TPD") unit as central core end-capped by two triazatruxene (or "TAT") units (**Fig. 1**). The TAT unit is a flat and highly soluble functionalized triazatruxene moiety that acts as a π-stacking platform. The four TPD-TAT molecules differ by the nature of the alkyl chains on TAT and TPD units, which are either linear or branched, as shown in **Fig. 1**. The TAT unit has three amine groups able to carry alkyl chains. Also, TPD can be alkylated independently from the TAT unit. Thus, different side-chain combinations were explored, with either 2-ethylhexyl (EH) branched side chains, *n*-octyl (C_8)

* emilie.steveler@insa-strasbourg.fr

linear side chains or a combination of both 2-ethylhexyl and *n*-octyl side chains[12, 13]. For example, TPD_{EH}-TAT_{C8} corresponds to the derivative with a branched side-chain on the TPD unit and linear side-chains on both TAT units (**Fig. 1**). Such molecules have been found to self-assemble into various solid-state phases, including liquid crystal mesophases and more ordered purely crystalline phases, under certain post-deposition treatments[12, 14].

In this work, steady-state photoluminescence (ST-PL) measurements were carried out in solution and in solid state. Time-resolved photoluminescence (TR-PL) measurements were carried out to investigate the exciton lifetime in TPD-TAT derivatives as a function of chemical structure and as a function of the solid-state structures. The results shown a significant increase in exciton lifetime with structural order. The relatively high exciton lifetime found here is consistent with the good performances obtained previously in solar cells using such molecules as efficient electron-donor in bulk heterojunctions solar cell[13].

2. RESULTS AND DISCUSSION

DSC combined with optical microscopy was used to study the thermal behavior of TPD-TAT derivatives with different side chains. As shown in **Fig. 1b**, branched side-chains (EH) on the TAT units (TAT_{EH}) lead to only a glass transition (*G*) at 75-80°C and a melting into an isotropic liquid states (I_{so}) at 80 °C. When linear side-chains (C_8) are grafted on the TAT (TAT_{C8}) units, significantly different thermal properties are observed. TDP-TAT_{C8} derivatives undergo a glass transition at 80 °C, and a cold crystallization from the fluid nematic phase (*N*) into a crystalline state (C_r), and finally melting in isotropic liquid state at around 180 °C. The cold crystallization occurs at 145 °C and 120 °C for TPD_{C8}-TAT_{C8} and TPD_{EH}-TAT_{C8}, respectively. Note that in the case of TPD-TAT molecules, the side-chains on the central chromophore TPD do not impact as much the thermal properties as do the side-chains on the TAT, pointing out that the molecular self-assembly is dominated by the planar TAT units[12]. These DSC results indicate specific heating conditions in the range of the fluid nematic phase to initiate a crystallization process of the bulk TPD_{C8}-TAT_{C8} material. Accordingly, annealing as-deposited layers at 145 °C causes the molecules to crystallize in the form of micrometer-sized needle-like crystals (as shown in **Fig. 1c**).

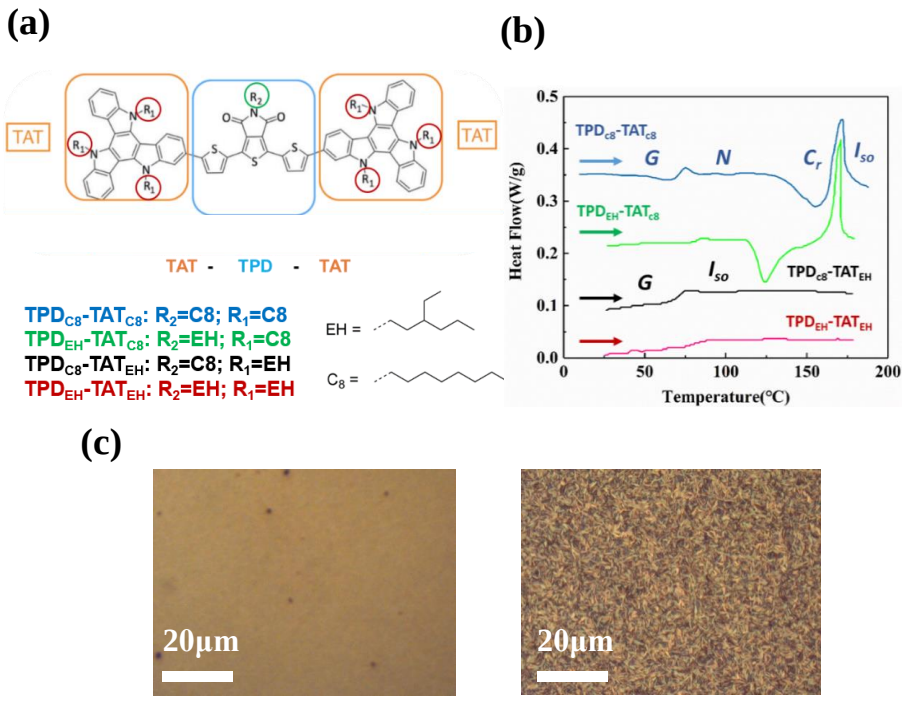

Figure 1 (a) Chemical structure of TPD-TAT derivatives. (b) DSC of TPD-TAT derivatives. (c) Different solid state of TPD_{C8}-TAT_{C8}, left: as-deposited, right: crystalline state.

Fig. 2 shows the ST-PL spectra and TR-PL transients measured for the four TPD-TAT derivatives in solution and in different solid-states. The ST-PL peak positions after gaussian deconvolution are summarized in **Table 1**. The four TPD-TAT derivatives in solution give rise to ST-PL spectra that are perfectly superimposed and split into mainly three vibronic peaks: a major emission band around 631 nm and two weak shoulders centered around 588nm and 650 nm (**Table 1**). The energy difference between the transitions being roughly constant, we may attribute the emission bands to 0-0 (588nm), 0-1 (631 nm) and 0-2 (650 nm) transitions[15-17].

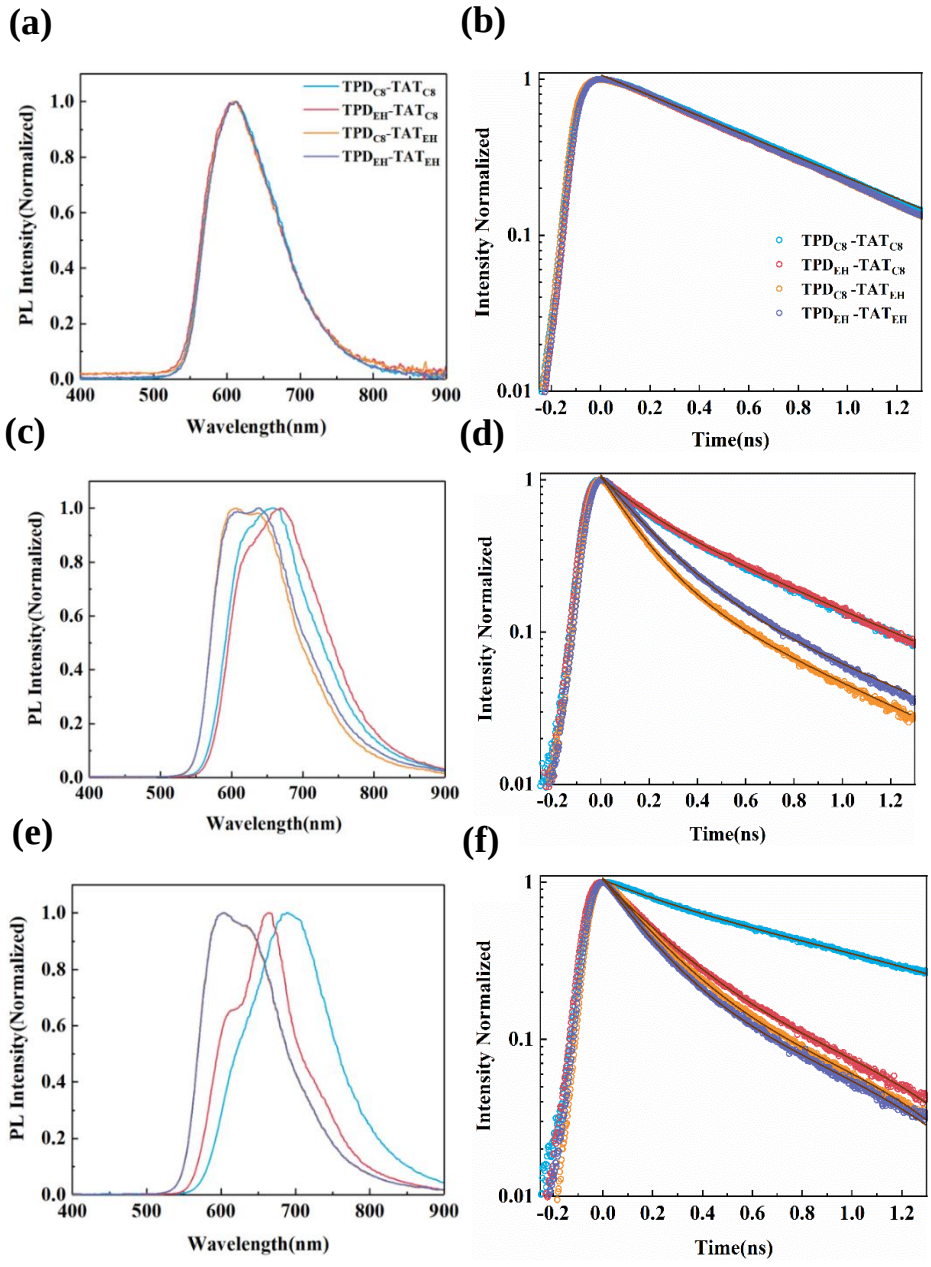

Figure 2 ST- PL and TR-PL for different TPD-TAT derivatives in solution (a) and (b), in as-deposited thin films (c) and (d), and in annealed thin films (e) and (f), respectively. In solution, TR-PL transients are fitted by a mono-exponential decay; in solid-state, TR-PL transients are fitted by a bi-exponential decay.

The TR-PL transients measured in solution (in the range from 650 to 700 nm) are also perfectly superimposed (**Fig. 1b**). Fitting the PL decay by a decreasing mono-exponential function gives rise to a unique exciton lifetime of 0.7 ns in solution (**Table 1**), indicating that the side-chains do not alter the molecular conformation, in agreement with the behavior observed for the ST-PL measurements.

Table 1 Positions of the PL peaks after deconvolution of the ST-PL spectra of TPD-TAT derivatives into three Gaussian peaks located at different wavelength (with error bar ±5nm).

States	Molecules	0-0 (nm)	0-1 (nm)	0-2 (nm)
Solution	TPD_{C8}-TAT_{C8} TPD_{EH}-TAT_{C8} TPD_{C8}-TAT_{EH} TPD_{EH}-TAT_{EH}	588	631	686
As-deposited	TPD_{C8}-TAT_{C8}	608	650	705
	TPD_{EH}-TAT_{C8}	608	660	712
	TPD_{C8}-TAT_{EH}	588	635	692
	TPD_{EH}-TAT_{EH}	588	635	692
Annealed	TPD_{C8}-TAT_{C8}	616	685	757
	TPD_{EH}-TAT_{C8}	605	660	695
	TPD_{C8}-TAT_{EH}	587	631	688
	TPD_{EH}-TAT_{EH}	587	631	688

Table 2 Photoluminescence lifetime of TPD-TAT derivatives in solution (0.5 mg/mL) and thin films (as-deposited and annealed). The lifetimes are obtained after a deconvolution of TR-PL transients with the instrument response function (IRF) and a fit with a mono-exponential function for solutions and with a bi-exponential function for thin films. For bi-exponential decays, the lifetime values are accompanied by that of their weight A_i in normalized spectra (A_1+A_2 =1). The values are given in ns and the error (noise, fit) is around ±0.05 ns.

	Solution $(A\,e^{-t/\tau})$	Thin film $(A_1\,e^{-t/\tau_1} + A_2\,e^{-t/\tau_2})$			
		As-deposited		Annealed	
TPD_{C8}-TAT_{C8}	0.70	$\tau_1 = 0.15$	$A_1 = 0.4$	$\tau_1 = 0.20$	$A_1 = 0.1$
		$\tau_2 = 0.60$	$A_2 = 0.6$	$\tau_2 = 1.05$	$A_2 = 0.9$
TPD_{EH}-TAT_{C8}		$\tau_1 = 0.15$	$A_1 = 0.4$	$\tau_1 = 0.20$	$A_1 = 0.6$
		$\tau_2 = 0.60$	$A_2 = 0.6$	$\tau_2 = 0.50$	$A_2 = 0.4$
TPD_{C8}-TAT_{EH}		$\tau_1 = 0.10$	$A_1 = 0.7$	$\tau_1 = 0.15$	$A_1 = 0.7$
		$\tau_2 = 0.40$	$A_2 = 0.3$	$\tau_2 = 0.50$	$A_2 = 0.3$
TPD_{EH}-TAT_{EH}		$\tau_1 = 0.15$	$A_1 = 0.6$	$\tau_1 = 0.10$	$A_1 = 0.7$
		$\tau_2 = 0.45$	$A_2 = 0.4$	$\tau_2 = 0.40$	$A_2 = 0.3$

In order to evaluate the impact of intermolecular interactions on the exciton lifetime, ST-PL and TR-PL experiments were performed on thin films for the four TPD-TAT derivatives. The measurements were done on either as-deposited or annealed films and are shown on **Fig. 2c and 2d**. The positions of the Gaussian peaks deconvoluted from the ST-PL spectra for as-deposited thin-films are summarized in the **Table 1**. As in solution, the shift in energy between the 0-1 and 0-0 transitions is approximately the same as that between the 0-1 and 0-2 transitions. In addition, the TPD-TAT_{C8} das-deposited thin films clearly show a significant red-shift of the transition bands in comparison to TPD-TAT_{EH}. This red-

shift indicates a stronger intermolecular coupling in the case of linear side-chains that should be beneficial for intermolecular charge and energy transfer[18, 19].

The TR-PL transients of as-deposited thin-films are shown in **Fig. 2d**. Although they are no more mono-exponential (see below), the slower decrease in PL for TPD-TAT_{C8} points out a longer exciton lifetime (**Table 2**) for these two derivatives in comparison to TPD-TAT_{EH}, but a shorter lifetime compared to the one measured in solution. The decrease in lifetime (in comparison to the reference value in solution) can be related to the intensity of intermolecular coupling in the solid-states. Strong π-stacking interactions do indeed often induce non-radiative recombination pathways that lead to a decrease in the exciton lifetime[20, 21]. Surprisingly, the results indicate that TPD-TAT_{C8} derivatives have a longer lifetime and thus a lower non-radiative recombination rate than TPD-TAT_{EH} derivatives despite the stronger intermolecular coupling revealed by the ST-PL. Moreover, the exciton lifetime is not significantly impacted by the side-chain nature (C_8 or EH) on the TPD unit. One possible reason is that the molecular self-assembly is mainly controlled by the side-chains on the TAT moieties, while the structural disorder in as-deposited films might be too high to allow the side-chain on the TPD unit to have an observable influence.

To compare the lifetimes more quantitatively, the TR-PL transients were fitted with a bi-exponential function. The results of the fit are presented in **Table 2** and confirm the qualitatively observed trend. The lifetime values show that the exciton lifetimes of the four as-deposited derivatives are roughly the same: a short lifetime of about 0.10-0.20 ns and a longer one around 0.45-0.60 ns. Interestingly, the weight of these components depends on the nature of the side- chains on the TAT units. For both TPD-TAT_{C8} derivatives, the higher lifetime is preponderant, but for both TPD-TAT_{EH} derivatives, the shorter one is leading the decay, resulting in a longer global PL decay for the TPD-TAT_{C8} derivatives, as observed on the TR-PL graphs.

Fig. 2e and 2f show the ST-PL and the TR-PL transients measured in annealed thin-films. The following annealing treatments: TPD_{C8}-TAT_{C8} were annealed at 145°C during 2h; TPD_{EH}-TAT_{C8} at 135°C during 2h; both TPD-TAT_{EH} at 145°C during 2h (The temperatures were chosen above the cold crystallization temperature according to the DSC results). The positions of the Gaussian peaks deconvoluted from the ST-PL spectra are presented in **Table 1**. Here again, for the TPD-TAT_{EH} annealed films, the energy gap between the transitions 0-1 and 0-0 is almost the same as between the transitions 0-2 and 0-1, and is in line with the previously obtained results. However, for TPD-TAT_{C8} annealed thin-films, the energy gap between the transitions 0-1 and 0-0 transitions is larger than that between the transitions 0-2 and 0-1. Moreover, ST-PL spectra of TPD_{C8}-TAT_{C8} shows a larger red-shift than TPD_{EH}-TAT_{C8} in their annealed thin-films. O. V. Mikhnenko *et al.* [22] observed a similar phenomenon in diketopyrrolopyrrole (DPP) derivatives for which the PL spectrum undergoes a gradual red-shift going from solution to as-deposited films and a further red-shift after annealing treatment. Such red-shifts could occur due to stronger intermolecular interactions in solid-states, which are enhanced upon annealing-induced crystallization[22]. Previously reported small angle X-ray scattering (SAXS) patterns reported by T. Han[12] *et al.* showed indeed that TPD_{C8}-TAT_{C8} thin films present higher crystallinity than TPD_{EH}-TAT_{C8} thin films.

The measured TR-PL transients show that the exciton lifetime decreases in TPD_{EH}-TAT_{C8} thin-film after annealing. Several reasons may a priori contribute to this behavior. On the one hand, thermal annealing results in the formation of crystalline domains that may lead to PL quenching at grain boundaries[22]. On the other hand, stronger π-stacking interactions in annealed thin-films induce non-radiative recombination pathways which may decrease the exciton lifetime as well. Interestingly, the TR-PL transients of TPD_{C8}-TAT_{C8} annealed thin-films (**Fig. 2f**) show significantly longer exciton lifetimes (**Table 2**) which even exceed the lifetime measured in solution. As shown in **Fig. 1c**, the derivative with both linear side-chains (C_8) on TAT and TPD units gives rise to self-assembled micrometric-sized crystalline needles after thermal treatment. The significantly larger average size of the crystals is likely to minimize exciton quenching at the grain boundaries. Also, the contribution of intra-grain defects acting as non-radiative recombination centers must be weak in order to allow the lifetime to exceed the reference value in solution[23-25]. The latter result is surprising, since the enhanced intermolecular coupling in the crystals, as revealed by high charge carrier mobility[14], does not translate into additional non-radiative pathways but rather the opposite. This behavior may be a consequence of the fact that the polar environment in the crystals could differ considerably from that in the solution. More advanced studies to elucidate the phenomena are on-going and will be reported elsewhere.

3. CONCLUSION

Through the investigation of the exciton lifetime for different chemical and self-assembly structures in TPD-TAT derivatives, we have shown that the side-chain nature on TPD and TAT units and the solid-states have a strong impact on their exciton lifetime. In particular, the exciton lifetime significantly increased from the as-deposited to the crystalline states, exceeding the lifetime measured in solution. These results may possibly be due to a decrease in the defect density in crystalline films (in comparison to as-deposited states) and to a different polar environment in the crystalline state resulting in lower non-radiative recombination rates. Importantly, the high intermolecular coupling in the molecular crystals of TPD_{C8}-TAT_{C8} does not favor non-radiative recombination. Rather, the large exciton lifetime combined with the previously reported high hole mobility for the same compound, shows that good charge transport does not necessarily hinder long exciton lifetimes. Also, strong intermolecular coupling combined with a long exciton lifetime should favor exciton diffusion and lead to rather long exciton diffusion lengths.

4. EXPERIMENTS

Thin film elaboration: The thin-films were deposited on quartz substrates from solution and submitted to various thermal treatments. The latter were selected to yield different solid-states. Thin-film deposition conditions and thermal processes were as follows:
(1) Substrates: quartz cleaned with liquid dish soap and sonicated in a series of deionized water, acetone, and isopropanol for 15 minutes each.
(2) UV-Ozone treatment: the substrates were treated in an UV-Ozone reactor for 30 minutes to eliminate any organic residues on the surface before spin-coating.
(3) Spin-coating thin-films: all solutions and thin-film preparation were done in a nitrogen filled glove box. Solutions were prepared at concentrations ranging from 1 to 20 mg/mL (for different thin-film thicknesses) with chloroform and left to stir overnight at room temperature. Solutions were spun onto the cleaned substrates with a deposition volume of 120 µL and a spin rate of 1500 rpm during 60 seconds.
(4) Thermal treatment: according to the DSC results, different annealing steps were applied to the TPD-TAT derivatives.
Steady-state photoluminescence: The samples (thin-films or solutions) were excited at 355 nm by a Nd-YAG laser, laser power is 88 mW, frequency is 15000 Hz, FWHM is 12.5 ns. Spectrometer used is a BRC112E CCD camera.
Time-resolved photoluminescence: all TR-PL measurements were carried out in atmospheric environment at room temperature. The samples were excited using a laser from Spectra-Physics Mai Tai. The beam characteristics are the following: a wavelength of 511 nm, a pulse duration of 90 ps, an energy per pulse of 0.05 nJ and a repetition rate of 20 MHz. TR-PL transients were measured using a Hamamatsu C6860 streak camera with a S-20 photocathode in synchro-scan mode. The full width half maximum (FWHM) of the instrument response function (IRF) is 40 ps.

5. ACKNOWLEDGEMENTS

J. Jing acknowledges financial support from China Scholarship Council (CSC).

REFERENCES

[1] Sajjad M. T., Ruseckas A. and Samuel I. D. W., "Enhancing Exciton Diffusion Length Provides New Opportunities for Organic Photovoltaics", Matter, 3, 341-354 (2020)
[2] Menke S. M., Luhman W. A. and Holmes R. J., "Tailored exciton diffusion in organic photovoltaic cells for enhanced power conversion efficiency", Nat. Mater, 12, 152-157 (2013)
[3] Hammed W. A., Yahya R., Bola A., Lukman u. and Mahmud H. N. M. E., "Recent Approaches to Controlling the Nanoscale Morphology of Polymer-Based Bulk-Heterojunction Solar Cells", Energies, 6, 5847-5868 (2013)
[4] Zhang Y., Liu K., Huang J., Xia X., Cao J., Zhao G., Fong P. W. K., Zhu Y., Yan F., Yang Y., Lu X. and Li G., "Graded bulk-heterojunction enables 17% binary organic solar cells via nonhalogenated open air coating", Nat. Commun., 12, 4815 (2021)
[5] Menke S. M., Luhman W. A. and Holmes R. J., "Tailored exciton diffusion in organic photovoltaic cells for enhanced power conversion efficiency", Nat. Mater, 12, 152-157 (2013)

[6] Lunt R. R., Giebink N. C., Belak A. A., Benziger J. B. and Forrest S. R., "Exciton diffusion lengths of organic semiconductor thin films measured by spectrally resolved photoluminescence quenching", J. Appl. Phys., 105, 053711 (2009)
[7] Xie X. and Ma H., "Opposite anisotropy effects of singlet and triplet exciton diffusion in tetracene crystal", ChemistryOpen, 5, 201 (2016)
[8] Coropceanu V., Cornil J., da Silva Filho D. A., Olivier Y., Silbey R. and Brédas J.-L., "Charge Transport in Organic Semiconductors", Chem. Rev., 107, 926-952 (2007)
[9] Chen F.-C., "Organic Semiconductors", Encyclopedia of Modern Optics (Second Edition), 220-231 (2018)
[10] Menke S. M. and Holmes R. J., "Exciton diffusion in organic photovoltaic cells", Energy Environ. Sci., 7, 499-512 (2014)
[11] Wong C. Y., Cotts B. L., Wu H. and Ginsberg N. S., "Exciton dynamics reveal aggregates with intermolecular order at hidden interfaces in solution-cast organic semiconducting films", Nat. Commun., 6, 1-7 (2015)
[12] Han T., Bulut I., Méry S., Heinrich B., Lévêque P., Leclerc N. and Heiser T., "Improved structural order by side-chain engineering of organic small molecules for photovoltaic applications", J. Mater. Chem. C, 5, 10794-10800 (2017)
[13] Bulut I., Chávez P., Mirloup A., Huaulmé Q., Hébraud A., Heinrich B., Fall S., Méry S., Ziessel R., Heiser T., Lévêque P. and Leclerc N., "Thiazole-based scaffolding for high performance solar cells", J. Mater. Chem. C, 4, 4296-4303 (2016)
[14] Jing J., Heinrich B., Prel A., Steveler E., Han T., Bulut I., Méry S., Leroy Y., Leclerc N., Lévêque P., Rosenthal M., Ivanov D. A. and Heiser T., "Efficient 3D charge transport in planar triazatruxene-based dumbbell-shaped molecules forming a bridged columnar phase", J. Mater. Chem. A, 9, 24315-24324 (2021)
[15] Spano F. C., Clark J., Silva C. and Friend R. H., "Determining exciton coherence from the photoluminescence spectral line shape in poly(3-hexylthiophene) thin films", J. Chem. Phys., 130, 074904 (2009)
[16] Long Y., Hedley G. J., Ruseckas A., Chowdhury M., Roland T., Serrano L. A., Cooke G. and Samuel I. D. W., "Effect of Annealing on Exciton Diffusion in a High Performance Small Molecule Organic Photovoltaic Material", ACS Appl. Mater. Interfaces, 9, 14945-14952 (2017)
[17] Ehrenreich P., Birkhold S. T., Zimmermann E., Hu H., Kim K.-D., Weickert J., Pfadler T. and Schmidt-Mende L., "H-aggregate analysis of P3HT thin films-Capability and limitation of photoluminescence and UV/Vis spectroscopy", Sci. Rep., 6, 32434 (2016)
[18] Oleson A., Zhu T., Dunn I. S., Bialas D., Bai Y., Zhang W., Dai M., Reichman D. R., Tempelaar R., Huang L. and Spano F. C., "Perylene Diimide-Based Hj- and hJ-Aggregates: The Prospect of Exciton Band Shape Engineering in Organic Materials", J. Phys. Chem, 123, 20567-20578 (2019)
[19] Marques S. R., Labastide J. A. and Barnes M. D., "Evolution of HJ Coupling in Nanoscale Molecular Self-Assemblies", The Journal of Physical Chemistry C, 122, 15723-15728 (2018)
[20] Menke S. M. and Holmes R. J., "Exciton diffusion in organic photovoltaic cells", Energy Environ. Sci., 7, 499-512 (2014)
[21] Ban M., Zou Y., Rivett J. P., Yang Y., Thomas T. H., Tan Y., Song T., Gao X., Credgington D. and Deschler F., "Solution-processed perovskite light emitting diodes with efficiency exceeding 15% through additive-controlled nanostructure tailoring", Nat. Commun., 9, 1-10 (2018)
[22] Mikhnenko O. V., Lin J., Shu Y., Anthony J. E., Blom P. W. M., Nguyen T.-Q. and Loi M. A., "Effect of thermal annealing on exciton diffusion in a diketopyrrolopyrrole derivative", Phys. Chem. Chem. Phys., 14, 14196-14201 (2012)
[23] Lin B., Zhou X., Zhao H., Yuan J., Zhou K., Chen K., Wu H., Guo R., Scheel M. A. and Chumakov A., "Balancing the pre-aggregation and crystallization kinetics enables high efficiency slot-die coated organic solar cells with reduced non-radiative recombination losses", Energy Environ. Sci., 13, 2467-2479 (2020)
[24] Forrest S. R., "Excitons and the lifetime of organic semiconductor devices", Philosophical Transactions of the Royal Society A: Mathematical, Physical and Engineering Sciences, 373, 20140320 (2015)
[25] Gerhard M., Louis B., Camacho R., Merdasa A., Li J., Kiligaridis A., Dobrovolsky A., Hofkens J. and Scheblykin I. G., "Microscopic insight into non-radiative decay in perovskite semiconductors from temperature-dependent luminescence blinking", Nat. Commun., 10, 1-12 (2019)